

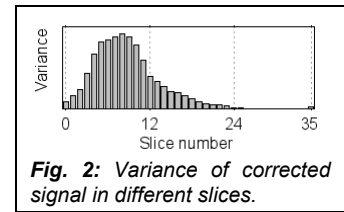
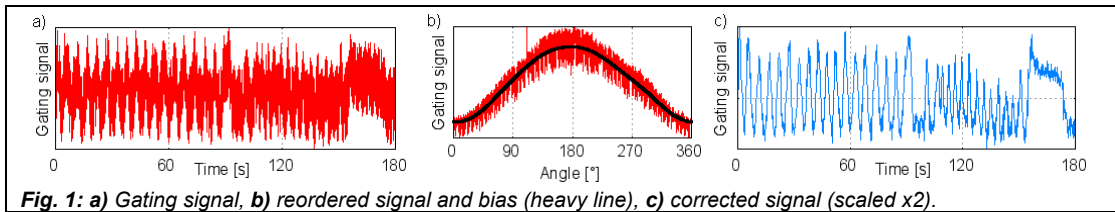
Bias Correction for Respiration Detection in Radial 3D Gradient-Echo Imaging

R. Grimm¹, K. T. Block², B. Kiefer², and J. Hornegger^{1,3}

¹Pattern Recognition Lab, Department of Computer Science, University of Erlangen-Nuremberg, Erlangen, Germany, ²Siemens Healthcare MR, Erlangen, Germany, ³Erlangen Graduate School in Advanced Optical Technologies (SAOT)

Introduction: Radial sampling of k-space is becoming an increasingly popular technique due to its inherent robustness to motion that eliminates the appearance of ghosting artifacts e.g. from respiratory motion. In addition, it has been shown that information about the respiratory cycle can be derived directly from the sampled data. This intrinsic property makes radial acquisitions very attractive for self-gated cardiac and abdominal imaging during free breathing. A commonly used trajectory is the “stack-of-stars” scheme with Cartesian slice encoding and radial sampling in the k_x - k_y plane [1]. Several self-gating signals that reflect the respiratory motion can be derived from the image data, e.g. the echo peak magnitude, or the center of mass along the slice direction [2,3,4], which is possible because all spokes run through the center of the center of mass. However, all these signals are rather sensitive to imperfections of the gradient timings [5] and, hence, the detected respiration pattern is often corrupted by an undesired dependency on the acquisition angle. Therefore, previous approaches [4,6] applied bandpass filters which sacrifices temporal resolution and implies regular breathing. In this work, a novel filtering scheme is described to reduce the angle-dependent signal fluctuations. It is shown that the proposed filter tolerates irregular breathing patterns and allows for an automatic selection of the slice delivering the most reliable gating signal. To evaluate the method, the corrected signal is used for a retrospective gating of a free-breathing liver scan where only data from a certain respiratory phase is employed for the reconstruction.

Materials and Methods: The proposed method is based on the golden-angle acquisition scheme where a fixed angular increment of 111.2° is applied [7]. This scheme has the advantage that the angle-dependent bias of the calculated signal presents as a high-frequency modulation that is separable from the rather slow respiratory cycle. Our filtering algorithm estimates and removes this angular bias. All of the previously mentioned self-gating signals can be used as input. Here, we use the image signal sum [4]. First, the gating values (Fig. 1a) are sorted according to the corresponding acquisition angle (Fig. 1b). The bias is then estimated by applying a Gaussian low-pass filter to the reordered data. Because the signal in the angular reordering is temporally incoherent as a result of the golden angle acquisition, this procedure does not affect the temporal resolution of the gating signal. The bias curve is then subtracted from the unfiltered data, and the corrected data is eventually resorted again into the original order (Fig. 1c).



Afterwards, the slice that delivers the most reliable gating signal is identified by finding the slice with the highest remaining variance in the corrected signal, assuming that higher deviations are expected in slices that are more severely affected by the respiratory motion. This step is, of course, only applicable for multi-slice acquisitions and for gating signals that can be computed independently for every slice. Here, we compute and analyze the variance of the slice k_x - k_y centers.

To evaluate the algorithm, in-vivo data from a healthy volunteer was acquired using a 1.5 T Siemens MAGNETOM Avanto (Siemens Healthcare, Erlangen, Germany) with a five-channel body coil. A radial VIBE sequence was used with the following parameters: TR/TE=4.15/1.97 ms, flip angle 10° , bandwidth 600 Hz/pixel, FOV 38x38x21.6 cm (320x320 imaging matrix, 36 slices), 960 radial spokes, TA 3 min (temporal resolution 187.5 ms per stack of spokes), golden ratio acquisition scheme. In order to validate the respiratory motion detection, the volunteer was instructed to exhale deeply once and then to breathe faster approximately at the middle of the measurement, followed by a short end-inhalation breath-hold.

Results and Discussion: Although a coarse trend of the breathing pattern can be guessed from the unprocessed gating signal (Fig. 1a), the exact locations of minima and maxima are obscured by the high-frequency variations caused by the angular bias. These distortions are significantly reduced in the corrected signal (Fig. 1c), allowing for a more stable detection of the gating points. The changes in the breathing pattern are clearly visible.

As shown in Fig. 1b, the scale of the bias can easily exceed the scale of the variations induced by the breathing. Therefore, the highest variance in an uncorrected gating signal may occur in a slice that is most affected by the bias instead of the one that reflects the breathing motion best. However, in the corrected signal, the highest variance is found in slice 8 in superior-inferior direction (Fig. 2). This slice corresponds to an axial cut through the diaphragm, which is indeed subject to significant respiratory motion. Reconstructions of slice 8 at the detected end-inspiration and end-expiration are shown in Fig. 3, where the corrected gating signal from this slice was used to define data acceptance windows. Slice 8 is indicated in red in Fig. 3c-d. When multiple receive coils are used, the coil element that is most suitable for gating can be identified by comparing the variances among the different channels, similar to the procedure described for finding slices that are strongly influenced by breathing motion.

Conclusion: We presented a filtering algorithm that reduces angle-dependent bias effects in self-gating signals while preserving the temporal resolution. The variance in the corrected signal indicates how much the signal reflects respiratory motion. Thus, a suitable slice for the calculation of the self-gating signal can be determined automatically.

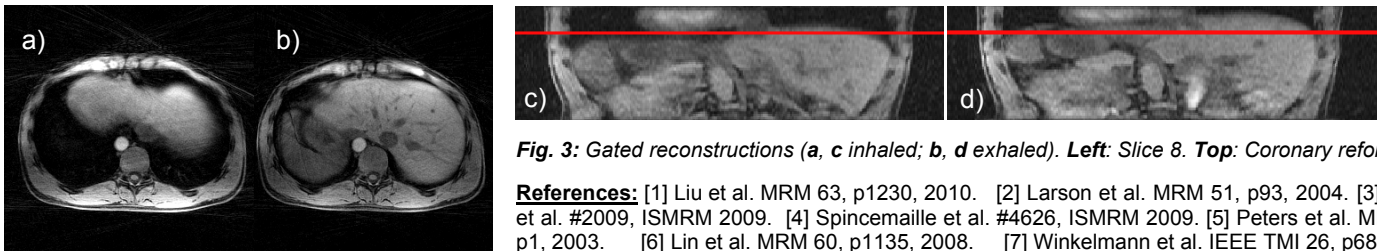


Fig. 3: Gated reconstructions (a, c inhaled; b, d exhaled). Left: Slice 8. Top: Coronary reformat.

References: [1] Liu et al. MRM 63, p1230, 2010. [2] Larson et al. MRM 51, p93, 2004. [3] Weick et al. #2009, ISMRM 2009. [4] Spincemille et al. #4626, ISMRM 2009. [5] Peters et al. MRM 50, p1, 2003. [6] Lin et al. MRM 60, p1135, 2008. [7] Winkelmann et al. IEEE TMI 26, p68, 2007.